DIPOLE STRENGTH FUNCTION IN ^{20}O

E. Tryggestad, T. Aumann,[a] D. Bazin, J. R. Beene,[b] Y. Blumenfeld,[c] M. Chartier,[d] M. L. Halbert,[e] P. Heckman, J. F. Liang,[f] D. C. Radford,[b] D. Shapira,[b] B. M. Sherrill, M. Thoennessen, and R. L. Varner[b]

The investigation of collective modes in unstable nuclei has recently become an important topic in the study of exotic nuclei. The isovector giant dipole resonance (GDR) is one of the most important and easily accessible of these collective modes. Theoretical calculations predict that GDR strength in neutron-rich nuclei will shift towards lower excitation energies as one probes closer to the neutron dripline [1,2]. As

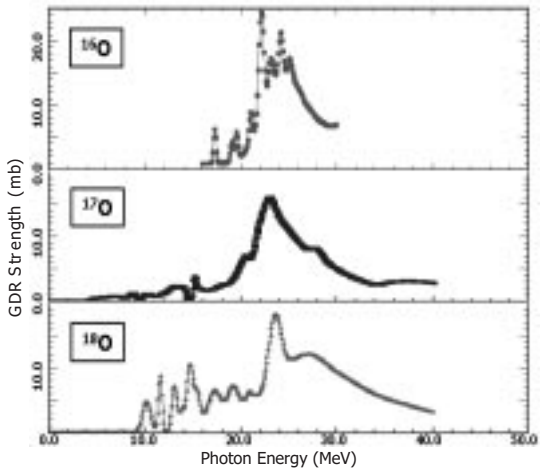

Figure 1: GDR strength distribution in oxygen isotopes measured by $(\gamma, x\mathrm{n})$ scattering. Significant strength is shifted towards lower energies for the neutron-rich isotopes (adapted from [3].)

an example, Figure 1 shows experimental $(\gamma, x\mathrm{n})$ scattering data for the β-stable oxygen isotopes ^{16,17,18}O [3]. Specifically, one can observe a relative increase of GDR strength at lower excitation energies in ^{18}O. The present experiment was performed to extend the scope of experimental knowledge regarding dipole strength in the oxygen isotopes. Studying neutron-rich ^{20}O, though, requires the use of radioactive beams and involves the excitation of the projectile rather than the target.

Two alternative experimental methods have been proposed, both of which rely on the Coulomb excitation of the projectile. The first of these is virtual photon absorption, where the excitation energy of the projectile is reconstructed knowing the energies of the break-up fragment and neutron(s) [4,5]. The second technique, explored in this study, is virtual photon scattering, a method which relies exclusively on projectile γ-ray decays [6]. Presently, low beam intensities constrain studies with neutron-rich, exotic nuclei, thereby limiting them to the light mass region. Therefore, the present experiment to measure the GDR strength function in ^{20}O also served as a test for the feasibility of the method.

The experimental method of virtual photon scattering can be treated as Coulomb excitation of the projectile followed by its subsequent ground-state photon decay [7,8]. The cross section for this process increases with the charge of the target and the beam energy of the projectile. In order to discriminate against nuclear processes it is necessary to limit detection of scattered projectiles to a small forward cone (selecting only large impact parameters).

There are two main differences between virtual photon absorption and virtual photon scattering. The absorption measurement cannot distinguish between different virtual photon multipolarities, whereas

the scattering experiments, with the requirement of observing ground state γ-ray decays, essentially limit the virtual spectrum to $E1$ multipolarity. The second difference is related to the neutron binding energy. As mentioned above, the absorption experiments rely on detection of neutrons for a kinematic reconstruction of the excitation energy and are therefore limited to probing strength functions above the neutron separation energy. In the scattering case, the cross section for ground-state γ-ray decay drops dramatically above the neutron binding energy. This effect, compounded further by low beam intensities, presently limits the realm of this method to excitation energies below the neutron binding energy. The neutron binding energy for ^{20}O lies at 7.608 MeV [9] which is sufficiently high to observe shifted, low-lying $E1$ strength.

A measurement was performed at the NSCL in October of 1998. A 10^6 pps, 100 MeV/u beam of ^{20}O (produced via fragmentation of ^{22}Ne on Be) was impinged on a 30 mg/cm^2 ^{208}Pb target. This target thickness was choosen as a compromise between maximizing event rate while limiting projectile energy straggling to ≈ 1 MeV FWHM. The scattered projectiles were analyzed with the S800 mass spectrometer which was operated in dispersion-matched mode. Using the S800, the inelastically-scattered^{20}O projectiles were fully-separated from other reaction fragments across a range in energy-loss of ≈ 40 MeV.

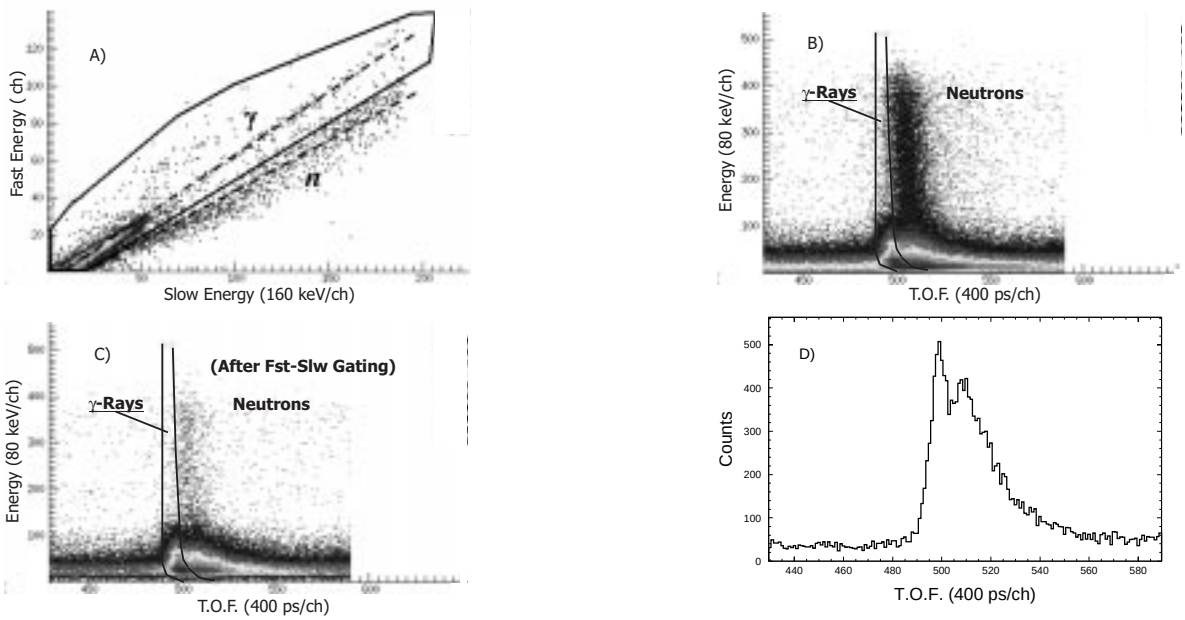

Figure 2: (A) Illustration of fast vs. slow gating. The deposited energy as detected with a short integration time (≈ 50 ns) is plotted against energy with a long integration time (≈ 1500 ns). (B) Time-of-flight (T.O.F.) is shown against deposited energy. (C) Same as (B) after fast vs. slow gating. (D) Projection of a 3.2–4.0 MeV energy cut from (C) on the T.O.F. axis.

In coincidence with the ^{20}O fragments, γ-rays were detected using 144 elements from the ORNL-TAMU-MSU BaF_2 array placed at forward angles surrounding the beam pipe, in a hexagonally-concentric orientation. The lab-frame angular coverage of the BaF_2 array was 11°–48°. For purposes of monitoring the contribution of target γ-rays to the overall yield, a smaller BaF_2 array (consisting of 7 elements) was placed at a backward location.

The placement of the detectors at very forward angles resulted in a large high-energy neutron background. Two methods where used in conjuction to suppress this neutron contamination. For neutrons depositing more than 3 MeV, "fast vs slow" gating could be applied (as shown in Figure 2(a)). This process

benefits from the component of fast ultraviolet light (subnanosecond) which is emitted by BaF_2 crystals during interactions with fast electrons and therefore is dependent on the type of incident radiation [10,11]. This fast component of light emitted by BaF_2 also allowed for a prompt timing measurement, which, when coupled with the precise projectile timing provided by two well separated (≈ 44 m) upstream multi-channel-plate timing detectors [12], faciliated further neutron supression via time-of-flight, see Figure 2(b,c,d).

For the selected γ-ray-coincident events, measured γ-ray energies were subjected to an add-back process, whereby energy deposited simultaneously in neighboring detectors was summed. This technique is necessary for the reconstruction of events where energy escapes detectors as a result of compton scattering and/or pair production. This technique improves the energy response of the array and the pile-up probability remains small due to the low multiplicity of multiple detector events. The summed γ-ray energy was then Doppler-corrected based on the scattering angle of the detector registering the largest energy deposition.

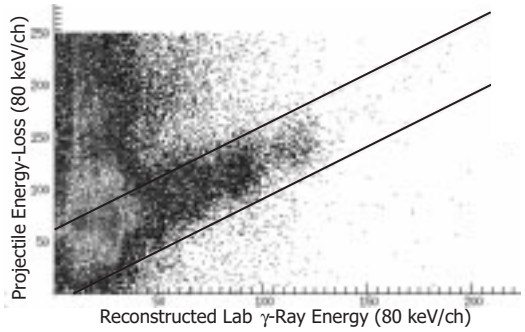

Figure 3: Final coincident event selection. Projectile energy-loss is shown against the reconstructed, lab-frame γ-ray energy. Events which are constrained by conservation of total energy fall on the diagonal.

The final event selection required correlating projectile inelastic energy-loss, as measured by the S800, with the reconstructed γ-ray energy as shown in Figure 3. Lying along the enhanced diagonal band are events where the energy-loss is equal to the γ-ray energy, thereby fulfilling the condition for virtual photon scattering.

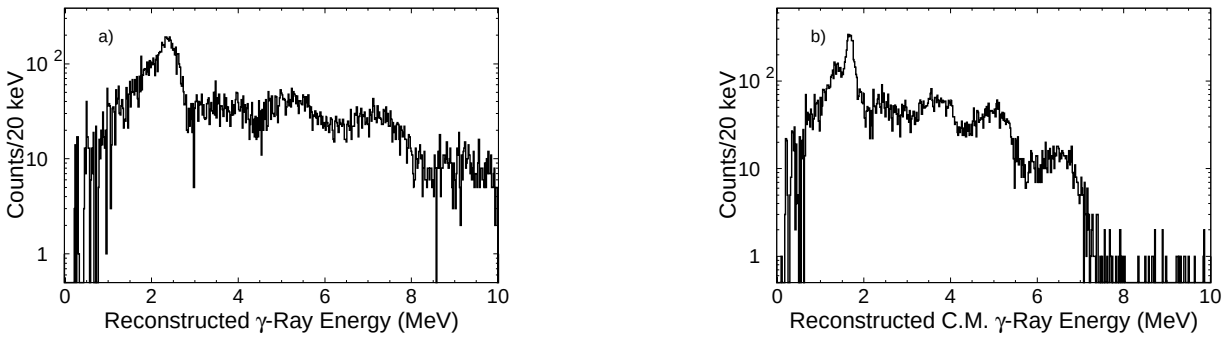

Figure 4: Reconstructed γ-ray energy spectra for all selected events: (a) represents lab-frame energy, while (b) is the Doppler-corrected equivalent. Several broad peaks are observed in the region beyond the predominant 2^+ transition at ≈ 1.7 MeV.

The preliminary results after final event-selection (the diagonal cut in Figure 3) are shown in Figure 4. This figure displays the reconstructed γ-ray energies, without (a) and with (b) Doppler correction.

The pronounced peak at ≈ 1.7 MeV results from the decay of the known first-excited 2^+ state [9]. The observation of this peak is evidence for correct identification of the projectile (^{20}O). Furthermore, the sharpening of this transition when comparing Figure 4(b) against (a) is a quantitative verification of the Doppler correction process.

Several broader peaks are observed above 3 MeV. We speculate that these structures result from $E1$ strength based on theoretical $B(E1)$ and $B(E2)$ information [13,14] and approximate Coulomb excitation cross section calculations for this energy region. These broad peaks cannot correspond to incorrectly Doppler-corrected, singular, sharp peaks because these structures are even broader in the non-Doppler-corrected spectrum. Current ^{20}O experimental data reveal no information regarding discrete 1^- states below the neutron separation energy [9].

Further analysis has to be performed to decisively determine the nature of these broad structures. For example, the shower multiplicity will show if the projectiles decay directly to the ground state (in support of $E1$ multipolarity) or if a cascade through one or more transition(s) occurs. Preliminary multiplicity investigations show that these are indeed direct ground-state transitions. GEANT [15] simulations will be performed to include the detector acceptances, efficiencies and responses.

a. GSI, Planckstr. 1, 64291 Darmstadt, Germany
b. Physics Division, Oak Ridge National Laboratory, Oak Ridge, TN 37831
c. IN_2P_3-CNRS, 91406 Orsay Cedex, France
d. CEN Bordeaux-Gradignan, BP 120, 33175 Gradignan Cedex, France
e. University of Tennessee, Knoxville, TN 37996
f. Oak Ridge Associated Universities, Oak Ridge, TN 37831

References

1. I. Hamamoto, H. Sagawa, and X. Z. Zhang, Phys. Rev. **C53** (1996) 765.
2. I. Hamamoto, and H. Sagawa, Phys. Rev. **C53** (1996) R1492.
3. S. S. Dietrich and B. L. Berman, At. Data Nucl. Tables, **38** (1988) 199.
4. T. Aumann, *et al.*, Nucl. Phys. **A649**, 297c (1999).
5. T. Aumann, *et al.*, Phys. Rev. **C59**, 1252 (1999).
6. R. L. Varner, *et al.*, Proc. Inter. Workshop on Collective Excitations in Fermi and Bose Systems, edited by C. Bertulani, World Scientific, p.264 (1999).
7. C. A. Bertulani and A. M. Nathan, Nucl. Phys **A554** (1993) 158.
8. R. L. Varner *et al.*, Proc. 2^{nd} Inter. Conf. on Exotic Nuclei and Atomic Masses, edited by B. M. Sherrill, D. J. Morrissey, and C. N. Davids, AIP Conference Proceedings **455**, p. 245 (1998).
9. D. R. Tilley *et al.*, Nucl. Phys **A636** (1998) 249.
10. M. Laval *et al.*, Nucl. Instr. and Meth. **206** (1983) 169.
11. R. Novotny *et al.*, Nucl. Instr. and Meth. **A262** (1987) 340.
12. D. Shapira and T. A. Lewis, to be published.
13. H. Sagawa and Toshio Suzuki, Phys. Rev. **C59** (1999) 3116.
14. E. Khan and Nguyen Van Giai, Phys. Lett. **B472** (2000) 253.
15. *Geant – Detector Description and Simulation Tool*, Application Software Group, Computing and Networks Division, CERN, Geneva, Switzerland (1993).